

# Discovery of “Molecular Switches” within a Series of mGlu<sub>5</sub> Allosteric Ligands Driven by a “Magic Methyl” Effect Affording Both PAMs and NAMs with *In Vivo* Activity, Derived from an M<sub>1</sub> PAM Chemotype

Lisa Barbaro, Alice L. Rodriguez, Ashlyn N. Blevins, Jonathan W. Dickerson, Natasha Billard, Olivier Boutaud, Jerri L. Rook, Colleen M. Niswender, P. Jeffrey Conn, Darren W. Engers, and Craig W. Lindsley\*



Cite This: *ACS Bio Med Chem Au* 2021, 1, 21–30



Read Online

ACCESS |



Metrics & More



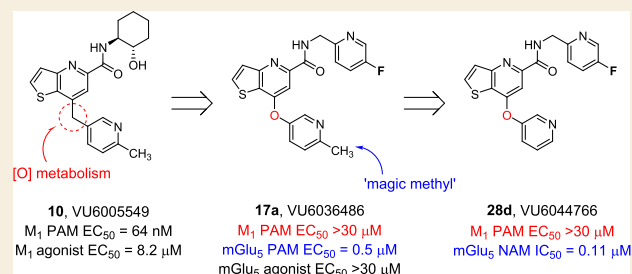
Article Recommendations



Supporting Information

**ABSTRACT:** In the course of optimizing an M<sub>1</sub> PAM chemotype, introduction of an ether moiety unexpectedly abolished M<sub>1</sub> PAM activity while engendering a “molecular switch” to afford a weak, pure mGlu<sub>5</sub> PAM. Further optimization was able to deliver a potent (mGlu<sub>5</sub> EC<sub>50</sub> = 520 nM, 63% Glu Max), centrally penetrant (K<sub>p</sub> = 0.83), MPEP-site binding mGlu<sub>5</sub> PAM 17a (VU6036486) that reversed amphetamine-induced hyperlocomotion. A pronounced “magic methyl” effect was noted with a regioisomeric methyl congener, leading to a change in pharmacology to afford a potent (mGlu<sub>5</sub> IC<sub>50</sub> = 110 nM, 3% Glu Min), centrally penetrant (K<sub>p</sub> = 0.94), MPEP-site binding NAM 28d (VU6044766) that displayed anxiolytic activity in a mouse marble burying assay. These data further support the growing body of literature concerning the existence of G protein-coupled receptor (GPCR) allosteric privileged structures, and the value and impact of subtle methyl group walks, as well as the highly productive fluorine walk, around allosteric ligand cores to stabilize unique GPCR conformations.

**KEYWORDS:** positive allosteric modulator (PAM), negative allosteric modulator (NAM), metabotropic glutamate receptor 5 (mGlu<sub>5</sub>), CNS penetration, structure–activity-relationship (SAR), privileged structure



## INTRODUCTION

G Protein-Coupled Receptors (GPCRs) are highly flexible membrane-bound proteins that are continuously sampling new active and inactive state ensembles with unique signaling profiles.<sup>1–4</sup> Allosteric ligands, both positive and negative allosteric modulators (PAMs and NAMs), are able to stabilize these unique receptor ensembles for therapeutic benefit, targeting less evolutionarily conserved binding (often induced-fit) sites, deep within the transmembrane binding domain.<sup>5–9</sup> We were the first to report on the phenomenon of “molecular switches” among allosteric ligands, wherein subtle structural changes to the ligand can induce significant changes in receptor–ligand interaction and/or receptor conformation leading to changes in the mode of pharmacology, i.e., PAM to NAM, or changes in family subtype selectivity, i.e., mGlu<sub>5</sub> PAM to mGlu<sub>3</sub> NAM.<sup>10–14</sup> More recently, and building on the classical concept of “privileged structures” of GPCR orthosteric ligands,<sup>15</sup> a similar concept is emerging for GPCR allosteric modulator ligands.<sup>16,17</sup> Here, we note two different concepts: (1) cooperativity-driven subtype selectivity, wherein an allosteric ligand binds to all members of a family but appears

to be a PAM of a single subtype due to high cooperativity with the orthosteric agonist (while other subtypes show neutral cooperativity) and (2) chemistry-driven pharmacology, where subtle changes to an mGlu<sub>5</sub> PAM ligand, for example, can lead to a potent mGlu<sub>3</sub> NAM ligand. Once recognized, it has become relatively straightforward to convert multiple mGlu<sub>5</sub> PAM chemotypes into mGlu<sub>3</sub> NAMs.<sup>13,14</sup>

Of the eight currently identified metabotropic glutamate receptors (mGlu<sub>1–8</sub>), mGlu<sub>5</sub> has received recent attention as a promising target for multiple CNS disorders and is one of the most studied, both preclinically and clinically.<sup>18,19</sup> Several mGlu<sub>5</sub> NAMs have advanced into human testing, demonstrating proof-of-concept in numerous CNS disorders; however, historical NAMs with little chemotype diversity have exhibited

Received: July 9, 2021

Published: August 20, 2021



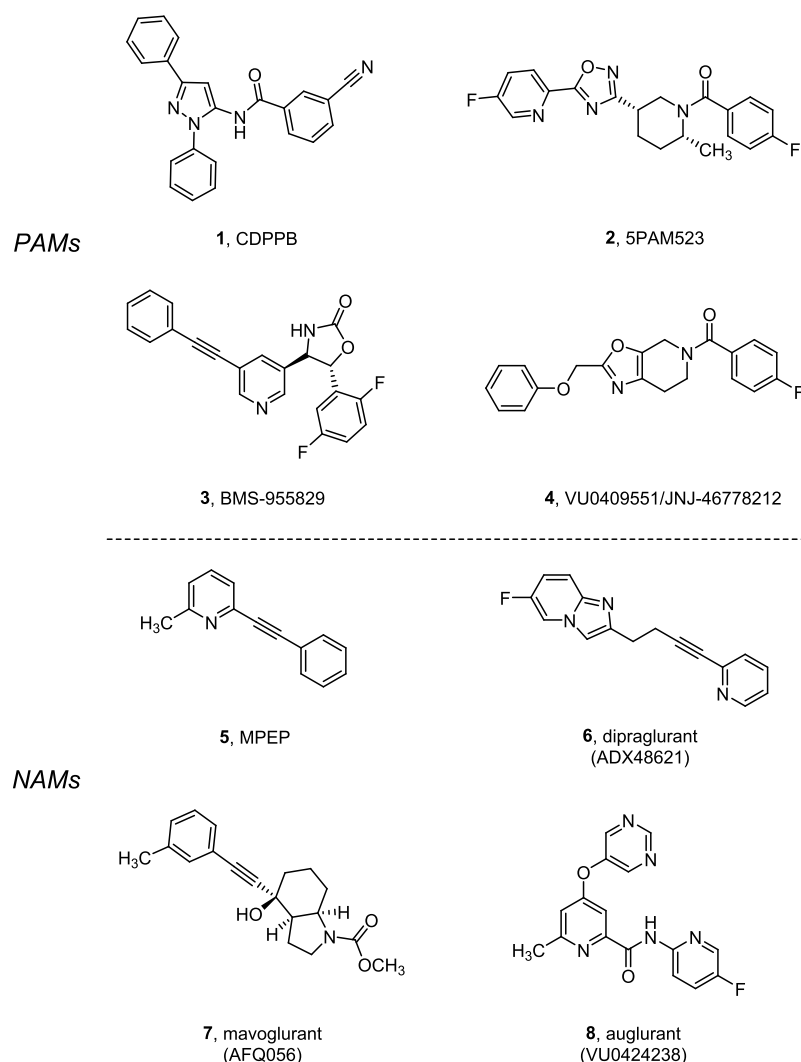


**Figure 1.** Structures of representative mGlu<sub>5</sub> PAMs (1–4) and NAMs (5–8) that have displayed *in vivo* efficacy.

narrow therapeutic windows and dose-limiting psychotomimetic-like effects.<sup>14,21</sup> Additionally, the prototypical heterobiaryl acetylene chemotype found in many of these compounds has long been associated with short half-life compounds and hepatotoxicity.<sup>20,21</sup> Thus, novel, nonacetylene chemotypes are in high demand. In contrast, mGlu<sub>5</sub>PAMs have proven more challenging and laden with pharmacological caveats (Figure 1).<sup>8,12</sup> Early on, it became clear that mGlu<sub>5</sub> ago-PAMs and PAMs with large fold-shifts displayed neurotoxicity in preclinical rodent models, despite robust antipsychotic and pro-cognitive efficacy; thus, “pure” PAMs, devoid of agonist activity, became the target of choice. Ultimately, signal bias afforded an approach to achieve the benefits of mGlu<sub>5</sub> PAMs without the adverse effect liability.

In this case, VU0409551, a novel mGlu<sub>5</sub> PAM, exhibited distinct stimulus bias and selectively potentiated mGlu<sub>5</sub> coupling to G<sub>αq</sub>-mediated signaling (but not mGlu<sub>5</sub> modulation of NMDAR currents or NMDAR-dependent synaptic plasticity in the rat hippocampus) and yielded robust antipsychotic-like and cognition-enhancing activity without neurotoxicity.<sup>22,23</sup> However, the VU0409551 scaffold is an exception, and our Center continues to search for new mGlu<sub>5</sub> PAM chemotypes devoid of agonism and with the potential for signal bias. Here, we detail efforts toward new mGlu<sub>5</sub>PAM and NAM chemotypes,

derived unexpectedly from an M<sub>1</sub> PAM scaffold,<sup>24</sup> and the impact of a “magic methyl”<sup>25–27</sup> as a “molecular switch” to provide centrally active mGlu<sub>5</sub> PAMs and NAMs within a highly conserved series of 7-alkoxy-thieno[3,2-*b*]pyridine-5-carboxamides.

## RESULTS AND DISCUSSION

A back-up lead optimization campaign for our M<sub>1</sub> PAM VU-319/ACP-319 program led to the in-depth profiling of numerous scaffolds in an effort to identify “pure” M<sub>1</sub> PAMs devoid of agonist activity and associated undesired cholinergic adverse events.<sup>24,28</sup> One such campaign identified a true “needle in the haystack” with VU6007477 (9) as a rare member of a series of M<sub>1</sub> PAMs based on a pyrrolo[2,3-*b*]pyridine carboxamide core that displayed no M<sub>1</sub> agonism and a lack of cholinergic toxicity; however, K<sub>p</sub> was modest and overall DMPK was modest to poor.<sup>24</sup> This led to a broader survey of alternate 5,6-heterobicyclic cores (Figure 2), and the identification of potent M<sub>1</sub> PAMs derived from a thieno[3,2-*b*]pyridine core, exemplified by VU6005549 (10). Amide scans of 10 led to numerous active moieties, yet the DMPK profiles were all unacceptable for further progression down the lead optimization flowchart. The benzylic CH<sub>2</sub> was shown to be a metabolic hotspot, but attempts to block this proved ineffective; therefore,

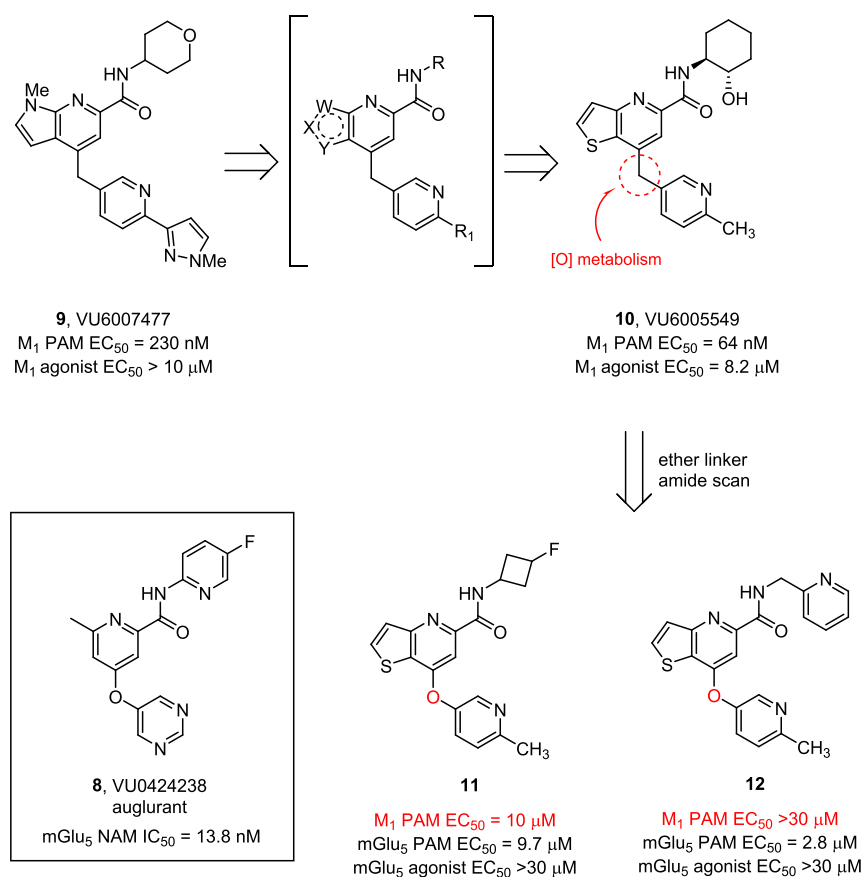
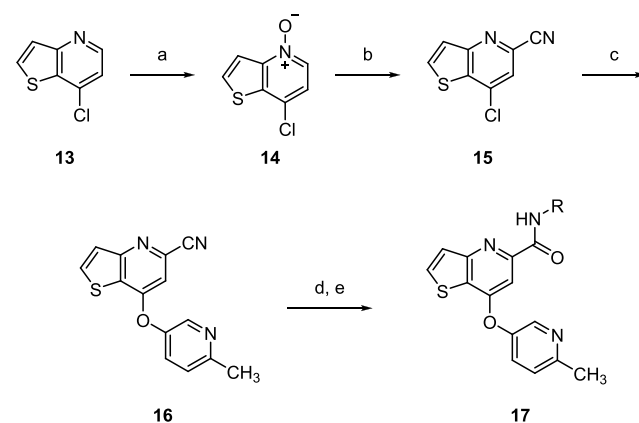


**Figure 2.** Optimization of an M<sub>1</sub> PAM **9** into a novel mGlu<sub>5</sub> PAM series (e.g., **12**) devoid of agonism, yet structurally similar to an mGlu<sub>5</sub> NAM (**8**), VU0424238 (auglurant).

we replaced the carbon linker with an oxygen atom to provide heterobiaryl ethers such as **11** and **12**. To our surprise, both **11** and **12** were inactive as M<sub>1</sub> PAMs; however, we recognized the chemotype as one having high homology with our prototypical mGlu<sub>5</sub> NAM (**13**), VU0424238 (**8**, auglurant).<sup>21</sup> Thus, we screened **11** and **12** in our mGlu<sub>5</sub> triple-add screening protocol (to simultaneously capture agonist, PAM and NAM activity), and both compounds proved to be weak mGlu<sub>5</sub> PAMs (EC<sub>50</sub>s of 9.7 and 2.8 μM, for **11** and **12**, respectively), with no agonist (EC<sub>50</sub> > 30 μM) activity. While this was not expected (an M<sub>1</sub> PAM switching to an mGlu<sub>5</sub> PAM), this result identified a new mGlu<sub>5</sub> PAM scaffold devoid of agonist activity.

To optimize mGlu<sub>5</sub> PAM **12**, we initially centered our efforts on evaluating the structure–activity relationship (SAR) in the northern amide region through incorporating a diverse array of methylene-linked heteroaryl rings, with particular focus in walking a variety of substituents (i.e., halogen, alkyl, etc.) around the ring. As depicted in **Scheme 1**, the synthesis of these amide analogues **17** was conducted in a straightforward fashion in 5-steps.<sup>29</sup> Starting from commercially available 7-chlorothieno[3,2-*b*]pyridine **13**, oxidation with *m*-CPBA provided the requisite *N*-oxide **14** to facilitate cyanation using trimethylsilyl cyanide and dimethylcarbonyl chloride. In the following step, the resulting intermediate **15** underwent microwave-assisted nucleophilic aromatic substitution with 5-hydroxy-2-methylpyridine, providing pyridyl-ether **16** in 82% yield. Desired analogs **17** were obtained following nitrile hydrolysis and standard amide formation (i.e., HATU) with a variety of commercially available aminomethylpyridines.

### Scheme 1. Synthesis of Amide Analogs **17**<sup>a</sup>



<sup>a</sup>Reagents and conditions: (a) *m*-CPBA, CH<sub>2</sub>Cl<sub>2</sub>, rt, 19 h, 92–98%; (b) Me<sub>3</sub>SiCN, Me<sub>2</sub>NCOCl, CH<sub>2</sub>Cl<sub>2</sub>, 44 h, 82%; (c) 5-hydroxy-2-methylpyridine, K<sub>2</sub>CO<sub>3</sub>, DMF, microwave 150 °C, 15 min, 78–82%; (d) conc. HCl, reflux, 1.5 h, 88%; (e) NH<sub>2</sub>R, HATU, DIPEA, DMF, 60 °C, 23–74%.

In short order, 24 synthesized amide derivatives **17** were screened using a calcium fluorescence “triple add” protocol which is able to simultaneously identify agonists, NAMs, and PAMs. The resulting SAR for this series was “shallow”, a common observation during optimization of allosteric modulators, with almost all analogs **17** devoid of mGlu<sub>5</sub> PAM activity<sup>22,23</sup> (see Supporting Information, **Table S1**). The only active compounds from this series resulted from the classic

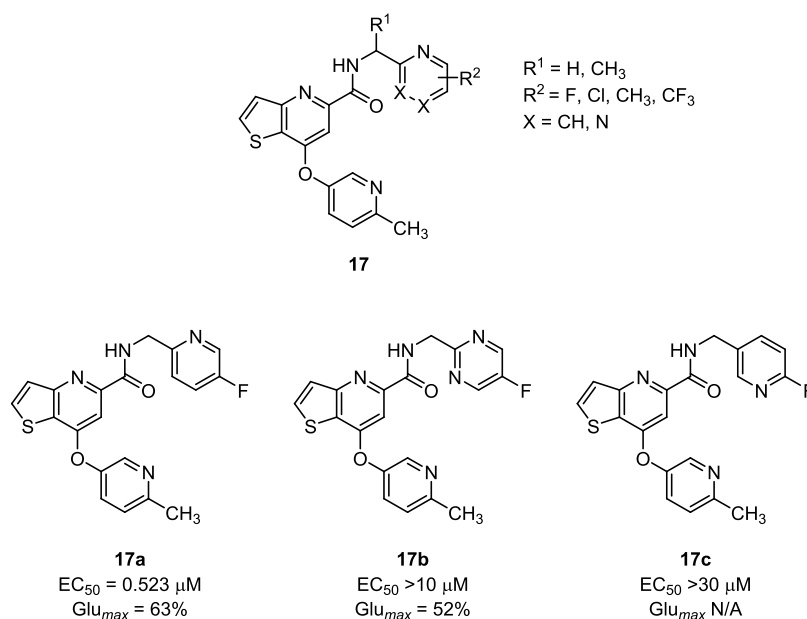
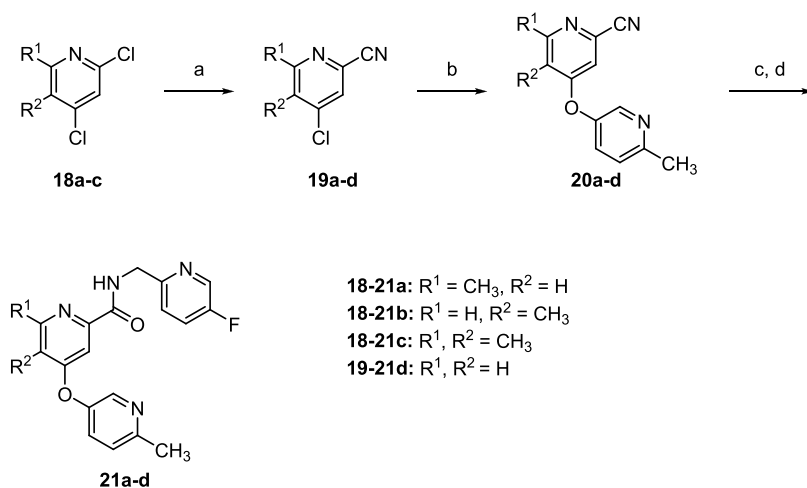


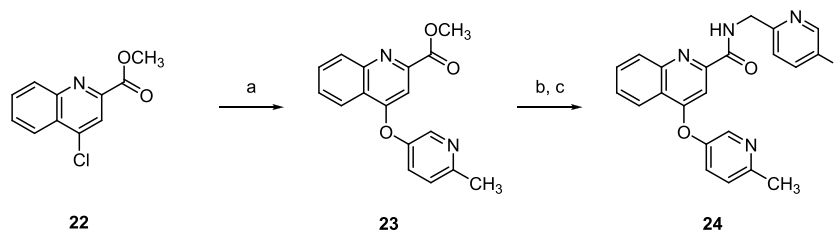
**Figure 3.** Summary of structural changes conducted in the methylpyridine region of hit compound **12**, with mGlu<sub>5</sub> activities of selected analogs **17**.

### Scheme 2. Synthesis of Pyridine Core Analogs **21**<sup>a</sup>



<sup>a</sup>Reagents and conditions: (a)  $\text{Zn}(\text{CN})_2$ ,  $\text{Pd}(\text{PPh}_3)_4$ , DMF, 120 °C, 2–4 h, 30–63% (b) 5-hydroxy-2-methylpyridine,  $\text{K}_2\text{CO}_3$ , DMF, microwave 150 °C, 15–30 min, 73–92% (c) conc. HCl, reflux; (d) (5-fluoropyridin-2-yl)methanamine, HATU, DIPEA, DMF, 50 °C, 24–56% (2-steps).

### Scheme 3. Synthesis of Quinoline Core Analog **24**<sup>a</sup>



<sup>a</sup>Reagents and conditions: (a) 5-hydroxy-2-methylpyridine,  $\text{K}_2\text{CO}_3$ , DMF, 100 °C, 2 h, 47%; (b) NaOH (2M), MeOH, reflux, 75 °C, 4 h (c) (5-fluoropyridin-2-yl)methanamine, HATU, DIPEA, DMF, 50 °C, 12% (2-steps).

“fluorine walk” (Figure 3), with substitution at the pyridine 5-position (**17a**) affording a 5-fold improvement in potency in comparison to hit compound **12** ( $EC_{50} = 0.532 \mu\text{M}$  vs  $EC_{50} = 2.83 \mu\text{M}$ , respectively). Keeping the 5-fluorine in place, we also investigated the effect of incorporating an additional nitrogen

atom into the ring (**17b**); however, this was unfavorable, as was changing the position of the pyridine nitrogen (**17c**). Given these results, compound **17a** was chosen as our new lead for further development.

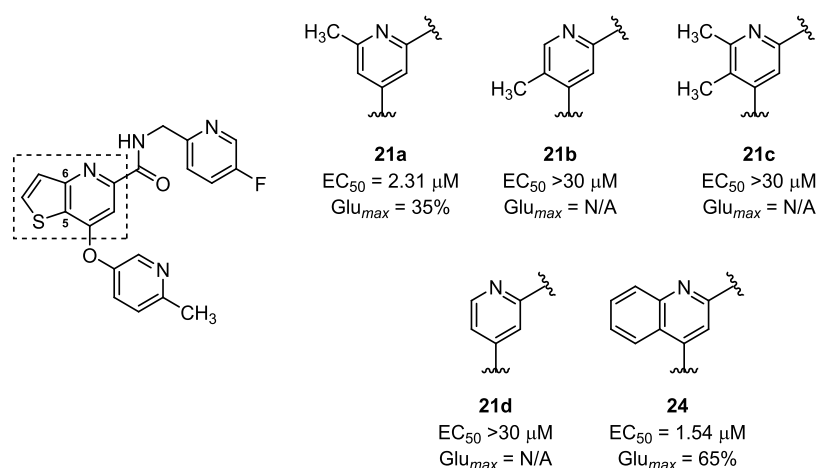
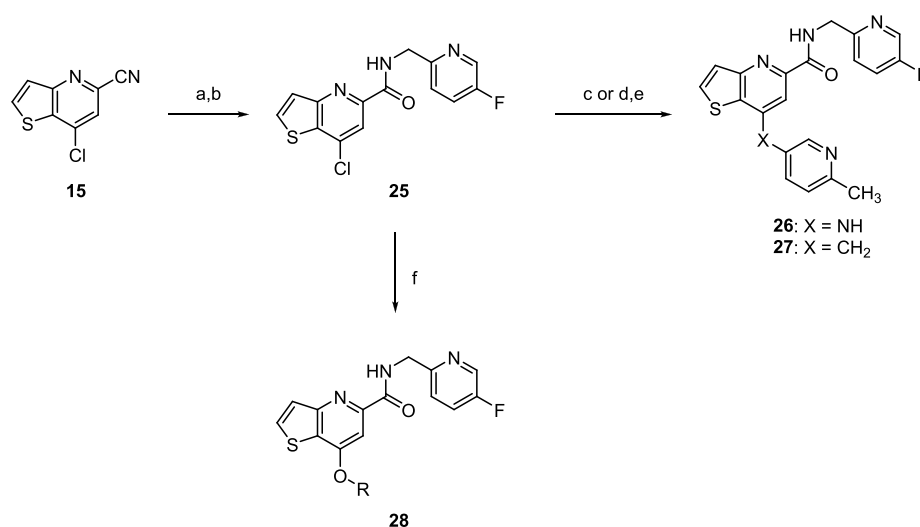


**Figure 4.** Summary of mGlu<sub>5</sub> activities of all synthesized core analogs **21** and **24**.

**Scheme 4.** Synthesis Analogs **26**, **27**, and **28**<sup>a</sup>



<sup>a</sup>Reagents and conditions: (a) conc. HCl, reflux, 1 h; (b) (5-fluoropyridin-2-yl)methanamine, HATU, DIPEA, DMF, 60 °C, 1–3 h, 29–55% (2-steps); (c) 5-amino-2-methylpyridine, Xantphos, Pd<sub>2</sub>(dba)<sub>3</sub>, Cs<sub>2</sub>CO<sub>3</sub>, 1,4-Dioxane, microwave 150 °C, 1.5 h, 53%; (d) B<sub>2</sub>pin<sub>2</sub>, PdCl<sub>2</sub>(PPh<sub>3</sub>)<sub>2</sub>, KOAc, 1,4-Dioxane, 100 °C, 1 h; (e) 5-(bromomethyl)-2-methyl-pyridine, Pd(dppf)Cl<sub>2</sub>·DCM, Cs<sub>2</sub>CO<sub>3</sub>, THF/H<sub>2</sub>O, 100 °C, 10 h (f) Pyridinol, KOtBu, DMSO, 70 °C, 10 h, 41% (2-steps).

In the next stage of our optimization protocol, we sought to explore changes to the central core of **17a**, with a particular focus on core truncation in an effort to identify the minimum required pharmacophore for mGlu<sub>5</sub> modulation. To prepare picolinamide derivatives **21a–d**, a nitrile was first installed to the core via palladium-catalyzed Negishi cross-coupling using the requisite dichloropyridine **18** and zinc cyanide (Scheme 2). From the resulting picolinonitriles **19**, including commercially available 4-chloropicolinonitrile, the remaining steps were analogous to those described for the synthesis of analogs **17** (*vide supra*). Alternatively, derivative **24** was prepared starting from the appropriate methyl ester **22**, followed by nucleophilic aromatic substitution, ester hydrolysis and amide coupling (Scheme 3).<sup>29</sup>

As shown in Figure 4, truncation of the core to the pyridine **21d** was met with a complete loss of activity, highlighting the importance of the bicyclic core for mGlu<sub>5</sub> modulation. Interestingly, activity was partially restored by the addition of a methyl group at the 6-position (**21a**); however, this was not observed with methyl substitution at the 5-position (**21b**) or with 5,6-disubstitution (**21c**). Additionally, the quinoline

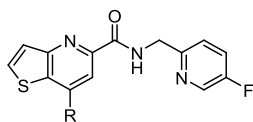
central core **24**, a common bioisostere of the thienopyridine, afforded good potency with similar efficacy to **17a**. While the central core SAR did provide alternative options, the original thienopyridine central core remained optimal.

In the final stage of our SAR exploration, we turned our attention to the southern pyridyl-ether region as another site of diversification. In addition to investigating alternate linker atoms in place of the ether, i.e., NH and CH<sub>2</sub>, we also investigated changes to the pyridine ring in this region by altering both the position of the methyl substituent as well as the position of the nitrogen. To prepare these derivatives, we modified our original synthetic strategy toward **17** (*vide supra*) to allow for late-stage exploration of the southern region (Scheme 4). Starting from nitrile **15**, hydrolysis followed by amide coupling provided intermediate **25** in good overall yield, which served as a common intermediate from which all analogs in this region were derived. The linker variants **26** and **27** were produced from **25** using either Buchwald-Hartwig cross-coupling with 5-amino-2-methylpyridine, or via Suzuki-Miyaura cross-coupling between the boronic ester of **25** and 5-(bromomethyl)-2-methyl-pyridine.

Alternatively, the pyridyl-ether analogs **28** were prepared using nucleophilic aromatic substitution with the requisite pyridinols.<sup>29</sup>

As shown in Table 1, changing the linker was not tolerated, with both linker variants **26** and **27** resulting in a significant loss

**Table 1. Structures and mGlu<sub>5</sub> Activities of Analogs 17a, 26, 27 and 28<sup>a</sup>**



Compound No.	R-group	mGlu <sub>5</sub> IC <sub>50</sub> (μM) <sup>a</sup>	%Glu min
<b>26</b>		>30	N/A
<b>27</b>		>30	N/A
<b>28a<sup>b</sup></b>		0.260	3
<b>28b<sup>b</sup></b>		0.203	2
<b>28c</b>		>30	N/A
<b>28d<sup>c</sup></b>		0.112	2
<b>28e</b>		1.9	80

<sup>a</sup>Calcium mobilization assays with HEK293 cells expressing human mGlu<sub>5</sub> performed in the presence of an EC<sub>80</sub> fixed concentration of glutamate; values represent the mean from one independent experiment performed in triplicate. <sup>b</sup>Values represent the mean from two ( $n = 2$ ) independent experiments performed in triplicate. <sup>c</sup>Values represent the mean from three ( $n = 3$ ) independent experiments performed in triplicate.

in activity. In contrast, very interesting results were obtained from the subtle modifications that were employed to the southern pyridine ring. Unexpectedly, almost all changes in this region engendered a “molecular switch”<sup>10–14</sup> to afford mGlu<sub>5</sub> NAMs by a regioisomeric “magic methyl” effect.<sup>25–27</sup> Most notably, removal of the 6-methyl substituent (**28d**) resulted in a potent NAM (IC<sub>50</sub> = 0.112 μM, 2% Glu<sub>max</sub>), as did moving the methyl substituent to the 3- and 4-positions (compounds **28a** and **28b**, respectively). In contrast, incorporating the methyl in the 2-position had deleterious effect on potency (**28c**). As has been noted in previous reports describing mGlu<sub>5</sub> allosteric ligands, such modulation resulting from slight perturbations in structure raises concerns over putative metabolites and their potential to engender opposing modes of mGlu<sub>5</sub> modulation. Additionally, shifting the pyridine nitrogen *ortho* relative to the

linker (**28e**) also provided an mGlu<sub>5</sub> NAM, however potency was significantly reduced in comparison to **28a**, **28b**, and **28d**.

Evaluation of the DMPK profiles of compounds **28a**, **28b**, and **28d** supported the selection of **28d** to progress into mouse behavioral studies given its slightly more favorable clearance and plasma protein binding (mCL<sub>hep</sub> = 82.4 mL/min/kg; mf<sub>u,p</sub> = 0.062) in comparison to those of **28a** (mCL<sub>hep</sub> = 85.1 mL/min/kg; mf<sub>u,p</sub> = 0.042) and **28b** (mCL<sub>hep</sub> = 86.5 mL/min/kg; mf<sub>u,p</sub> = 0.046).<sup>29</sup>

### Primary *in vitro* pharmacology and DMPK of PAM 7a and NAM 28d

On the basis of these exciting results, both PAM **17a** (VU6036486) and NAM **28d** (VU6044766) were progressed for further profiling in order to assess their potential as *in vivo* tool compounds (Table 2). In addition to potent activity at mGlu<sub>5</sub>, both compounds were found to demonstrate functional selectivity over the other mGlu receptors (mGlu<sub>1–4,7,8</sub> > 30 μM). To determine whether these compounds interacted at the common 2-methyl-6-(phenylethynyl)-pyridine (MPEP) allosteric binding site, displacement studies were conducted using

**Table 2. Summary of *In Vitro* Pharmacology and DMPK Data for Compounds 17a and 28d**

Property	PAM 17a	NAM 28d
<b>Physicochemical</b>		
MW	394	380
cLogP	2.41	2.22
tPSA	77	77
<b><i>In vitro</i> Pharmacology</b>		
hmGlu <sub>5</sub> EC <sub>50</sub> (μM)	0.52	N/A
hmGlu <sub>5</sub> IC <sub>50</sub> (μM)	N/A	0.11
mGlu <sub>5</sub> K <sub>i</sub> (μM)	>10	0.16
<b><i>In vitro</i> PK</b>		
CL <sub>int</sub> (mL/min/kg)		
Rat	152	314
Mouse	ND	970
Human	173	47.0
CL <sub>hep</sub> (mL/min/kg)		
Rat	47.8	57.2
Mouse	ND	82.4
Human	18.7	14.5
f <sub>u,p</sub>		
Rat	0.048	0.115
Mouse	ND	0.062
Human	0.056	0.068
Rat f <sub>u,b</sub>	0.030	0.035
<b><i>In vivo</i> Brain Distribution</b>		
Rat IV PBL cassette		
K <sub>p</sub>	0.83 <sup>a</sup>	0.94 <sup>b</sup>
K <sub>p,un</sub>	0.52 <sup>a</sup>	0.29 <sup>b</sup>
<b><i>In vivo</i> PK</b>		
IV dose (mg/kg)	0.2 (rat)	1.0 (mouse)
CL <sub>p</sub> (mL/min/kg)	36.9	141
V <sub>ss</sub> (L/kg)	2.20	8.2
Elim. t <sub>1/2</sub> (h)	1.37	0.69
PO dose (mg/kg)	10 (rat)	10 (mouse)
C <sub>max</sub> (ng/mL)	152	ND
t <sub>max</sub> (h)	0.50	ND
AUC <sub>inf</sub> (h*ng/mL)	371	ND
F (%)	8.22	ND

<sup>a</sup>0.20 mg/kg dose. <sup>b</sup>0.25 mg/kg dose.

the radioligand [ $^3\text{H}$ ]3-methoxy-5-pyridin-2-ylethynylpyridine ([ $^3\text{H}$ ]methoxyPEPy) which is a close structural analog of MPEP. As illustrated in Figure 5, the mGlu<sub>5</sub> NAM 28d

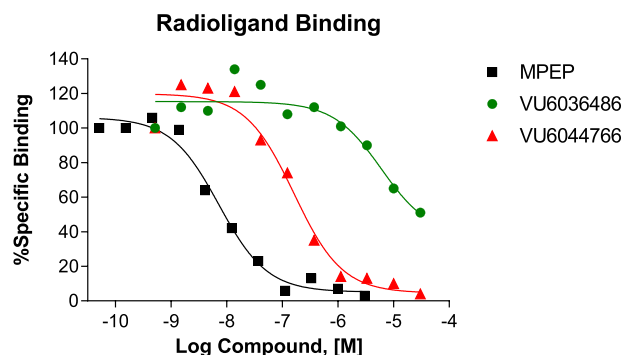


**Figure 5.** Radioligand competition binding experiments with 17a (VU6036486), 28d (VU6044766), and [ $^3\text{H}$ ]-3-methoxy-5-(pyridin-2-ylethynyl)pyridine, showing an interaction with the classical MPEP allosteric site on mGlu<sub>5</sub> ( $n = 1$ ).

(VU6044766) induced full displacement of radioligand binding, suggesting an interaction with the allosteric MPEP site ( $K_i = 0.16 \mu\text{M}$ ). Interestingly, PAM 17a (VU6036486) exhibited weak binding at concentrations up to  $100 \mu\text{M}$ , indicating an interaction at either the classical MPEP binding site and/or an alternative overlapping site.<sup>22,23</sup>

As shown in Table 2, compounds 17a and 28d were found to have good free fraction in plasma ( $f_{u,s} > 0.05$ ) and in brain ( $f_{u,s} > 0.03$ ); however, they were predicted to have high hepatic clearance across all species tested. The CNS penetration of both compounds was assessed using a rat plasma/brain level (PBL) cassette assay which revealed good exposure in brain for both PAM 17a ( $K_p = 0.83$ ,  $K_{p,uu} = 0.52$ ) and NAM 28d ( $K_p = 0.94$ ,  $K_{p,uu} = 0.29$ ). These data prompted further evaluation of discrete IV and PO pharmacokinetics for both compounds. PAM 17a displayed moderate clearance ( $36.9 \text{ mL/min/kg}$ ), a half-life of 1.37 h with a moderate volume of distribution ( $2.2 \text{ L/kg}$ ). Despite the promising *in vivo* data, the compound had low oral bioavailability (8%). For NAM 28d, the *in vivo* mouse study revealed superhepatic clearance ( $141 \text{ mL/min/kg}$ ), a half-life of 0.69 h and a high volume of distribution ( $8.2 \text{ L/kg}$ ). Of note,

there was no measurable drug in blood following mouse PO administration.<sup>29</sup>

### In Vivo Pharmacology

With a relatively potent mGlu<sub>5</sub> PAM (17a) and NAM (28d) with acceptable PK profiles and brain exposure, we were now poised to determine if the mGlu<sub>5</sub> modulation observed in our *in vitro* cellular assays would be mirrored by *in vivo* behavioral studies. To evaluate PAM 17a, we assessed its ability to reverse amphetamine-induced hyperlocomotion (AHL) which is used as a predictor of antipsychotic activity.<sup>22,23</sup> In this study, PAM 17a (VU6036486) was administered as a 30 or 60 mg/kg i.p. dose 30 min prior to a 0.75 mg/kg s.c. dose of amphetamine. As shown in Figure 6, PAM 17a reversed AHL by  $\sim 30\%$  at a dose of 60 mg/kg.<sup>29</sup>

To assess NAM 28d, we employed a marble burying assay to evaluate anxiolytic activity. Naive mice are well-known to bury foreign objects, e.g., glass marbles, in deep bedding.<sup>21</sup> This behavior can be inhibited with pretreatment of low doses of certain benzodiazepines or selective serotonin reuptake inhibitors and has also been proven to be sensitive to a diverse array of mGlu<sub>5</sub> NAM chemotypes.<sup>21</sup> As shown in Figure 7, a 30 mg/kg i.p. dose produced a significant reduction in marble burying relative to the vehicle-treated group, suggesting anxiolytic activity.<sup>27</sup>

### CONCLUSION

In summary, we have described the multidimensional optimization of a novel mGlu<sub>5</sub> PAM and mGlu<sub>5</sub> NAM chemotype based on a thieno[3,2-*b*]pyridine core scaffold, derived from an M<sub>1</sub> PAM ligand. Despite “shallow” SAR for the majority of our campaign, modification to the northern amide region effected a 5-fold improvement in potency of the original initial hit 2, resulting in compound 17a (VU6036486,  $\text{EC}_{50} = 0.52 \mu\text{M}$ ). Most interestingly, “molecular switches” were discovered through slight structural modifications to the southern pyridyl-ether region, resulting in the discovery of multiple mGlu<sub>5</sub> NAMs, the most potent being compound 28d (VU6044766,  $\text{IC}_{50} = 0.11 \mu\text{M}$ ). This report highlights that “molecular switches” can result from small structural changes, such as a “magic methyl”, and thus highlights the need to thoroughly investigate and develop chemical SAR as well as characterize metabolites of mGlu<sub>5</sub> allosteric ligands as these may

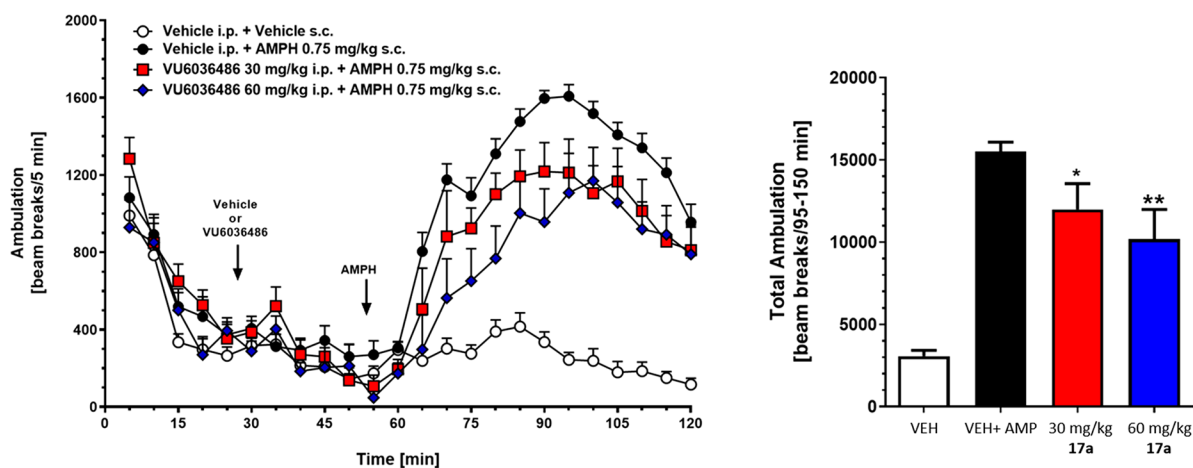


**Figure 6.** Dose-dependent reversal of amphetamine-induced hyperlocomotion in rats by PAM 17a;  $n = 7-8$  male Sprague–Dawley rats per treatment group; vehicle = 10% Tween 80 in  $\text{H}_2\text{O}$ ;  $*p < 0.05$ ,  $**p < 0.01$  vs vehicle/amphetamine (AMPH) control group.

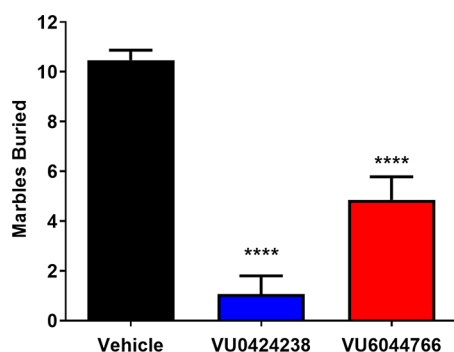


**Figure 7.** Inhibition of marble burying with NAM 28d (VU6044766) administered at a dose of 30 mg/kg;  $n = 14$  male CD-1 mice per treatment group; 15 min pretreatment, 30 min burying time; vehicle = polysorbate 80 (IP); \* $p < 0.05$  versus vehicle control group. VU0424238 was used as a positive control and administered at a dose of 30 mg/kg.

result in opposing modes of pharmacology. Finally, these data further strengthen the position that there are GPCR allosteric privileged structures and that these scaffolds can be employed to access allosteric ligands for multiple GPCR targets.

## EXPERIMENTAL SECTION

### Chemistry

All compounds were purified to  $\geq 95\%$  as determined by analytical LCMS (214 nm, 254 nm and ELSD) as well as  $^1\text{H}$  and  $^{13}\text{C}$  NMR and HRMS. The general chemistry, experimental information, and syntheses of all other compounds, along with detailed pharmacology, and DMPK methods are supplied in the [Supporting Information](#).

#### 7-Chlorothieno[3,2-*b*]pyridine 4-oxide (14)

To a solution of 7-chlorothieno[3,2-*b*]pyridine (2.00 g, 11.8 mmol) in dichloromethane (50 mL) was added 3-chloroperoxybenzoic acid (3.17 g, 14.2 mmol) in equal portions over a 5 min period. After 19 h at room temperature, a solution of  $\text{Na}_2\text{S}_2\text{O}_3$  (10% aqueous) was added to the reaction, and the organic layer was separated and washed with a solution of  $\text{K}_2\text{CO}_3$  (10% aqueous). The aqueous layer was extracted with dichloromethane (3x), and the combined organic layers washed with brine, dried over  $\text{Na}_2\text{SO}_4$  (anhydrous), filtered, and concentrated under reduced pressure to afford the title compound as a pale-yellow solid, which was used in the following step without further purification (2.12 g, 11.0 mmol, 93% yield).  $^1\text{H}$  NMR (400 MHz,  $\text{CDCl}_3$ )  $\delta = 8.26$  (d,  $J = 6.7$  Hz, 1H), 7.87 (d,  $J = 5.7$  Hz, 1H), 7.75 (d,  $J = 5.7$  Hz, 1H), 7.23 (d,  $J = 6.7$  Hz, 1H).  $^{13}\text{C}$  NMR (101 MHz,  $\text{CDCl}_3$ )  $\delta = 147.1$ , 136.4, 136.0, 131.7, 126.8, 120.1, 120.0. LC-MS (ESI+):  $R_T = 0.432$  min, 97% at 215 nm and  $>98\%$  at 254 nm,  $m/z = 186.3$  [M + H] $^+$ . HR-MS (TOF, ESI+): for  $\text{C}_7\text{H}_4\text{ClNOS}$  [M], calc'd 185.9775 [M + H] $^+$ , found 185.9770.

#### 7-Chlorothieno[3,2-*b*]pyridine-5-carbonitrile (15)

To a solution of 14 (2.11 g, 11.3 mmol) in dichloromethane (50 mL) was added trimethylsilyl cyanide (2.80 mL, 22.7 mmol). After 15 min at room temperature, dimethylcarbamoyl chloride (2.00 mL, 22.7 mmol) was added dropwise. After 19 h at room temperature, an additional amount of trimethylsilyl cyanide (2.80 mL, 22.7 mmol) and dimethylcarbamoyl chloride (2.00 mL, 22.7 mmol) were added. After a total of 44 h, a solution of  $\text{K}_2\text{CO}_3$  (10% aqueous) was added to the reaction mixture, and the organic layer separated. The aqueous layer was extracted with dichloromethane (3x), and the combined organic layers were washed with brine, dried over  $\text{Na}_2\text{SO}_4$  (anhydrous), filtered, and concentrated under reduced pressure. Purification by silica-gel flash chromatography (0–10% EtOAc/hexanes) afforded the title compound as a pale-yellow solid (1.86 g, 9.26 mmol, 82% yield).  $^1\text{H}$  NMR (400 MHz,  $\text{CDCl}_3$ )  $\delta = 7.99$  (d,  $J = 5.5$  Hz, 1H), 7.69–7.62 (m, 2H).  $^{13}\text{C}$  NMR (101 MHz,  $\text{CDCl}_3$ )  $\delta = 157.6$ , 139.3, 136.3, 134.4, 131.6,

126.0, 122.0, 116.9. LC-MS (ESI+):  $R_T = 0.762$  min, 97% at 215 nm and 98% at 254 nm,  $m/z = 195.3$  [M + H] $^+$ . HR-MS (TOF, ESI+): for  $\text{C}_8\text{H}_3\text{ClN}_2\text{S}$  [M], calc'd 194.9778 [M + H] $^+$ , found 194.9776.

#### 7-((6-Methylpyridin-3-yl)oxy)thieno[3,2-*b*]pyridine-5-carbonitrile (16)

To a microwave vial were added 15 (1.00 g, 5.14 mmol), 3-hydroxy-6-methylpyridine (0.673 g, 6.17 mmol), potassium carbonate (1.49 g, 10.8 mmol), and DMF (15 mL). The vial was capped and irradiated in a microwave reactor at 150 °C for 15 min. Upon completion, the reaction was diluted with water and dichloromethane, passed through a phase separator washing with dichloromethane (3x), and the collected organic phase was concentrated to dryness. Purification by silica-gel flash chromatography (0–50% EtOAc/hexanes) afforded the title compound as a white powder (1.15 g, 4.21 mmol, 82% yield).  $^1\text{H}$  NMR (400 MHz, MeOD)  $\delta = 8.48$  (d,  $J = 2.7$  Hz, 1H), 8.21 (d,  $J = 5.5$  Hz, 1H), 7.75 (dd,  $J = 8.5$ , 2.9 Hz, 1H), 7.62 (d,  $J = 5.5$  Hz, 1H), 7.51 (d,  $J = 8.5$  Hz, 1H), 7.13 (s, 1H), 2.63 (s, 3H).  $^{13}\text{C}$  NMR (101 MHz, MeOD)  $\delta = 161.6$ , 160.7, 157.9, 149.9, 142.3, 135.9, 133.6, 131.7, 127.0, 126.7, 125.8, 118.2, 109.0, 23.2. LC-MS (ESI+):  $R_T = 0.604$  min,  $>98\%$  at 215 and 254 nm,  $m/z = 268.4$  [M + H] $^+$ . HR-MS (TOF, ESI+): for  $\text{C}_{14}\text{H}_{13}\text{N}_3\text{OS}$  [M], calc'd 268.0539 [M + H] $^+$ , found 268.0538.

#### *N*-(5-Fluoropyridin-2-yl)methyl-7-((6-methylpyridin-3-yl)oxy)thieno[3,2-*b*]pyridine-5-carboxamide (17a, VU6036486)

**Step 1.** A mixture of compound 16 (2.05 g, 7.67 mmol) and concentrated HCl (37% aqueous, 75.6 mmol) was heated at 100 °C for 1.5 h. After the heat was removed, the reaction was neutralized with NaOH (6 M, aqueous) at room temperature, and the water and solvent were removed under reduced pressure. The crude residue was dissolved in 10% MeOH/DCM, the undissolved salt was filtered, and the collected filtrate was concentrated under reduced pressure to afford the title compound as an off-white solid, which was used in following step without further purification (2.01 g, 6.74 mmol, 88% yield).  $^1\text{H}$  NMR (400 MHz, DMSO)  $\delta = 8.53$  (d,  $J = 2.9$  Hz, 1H), 8.31 (d,  $J = 5.5$  Hz, 1H), 7.77 (dd,  $J = 8.5$ , 2.9 Hz, 1H), 7.74 (d,  $J = 5.5$  Hz, 1H), 7.45 (d,  $J = 8.5$  Hz, 1H), 7.15 (s, 1H), 2.55 (s, 3H).  $^{13}\text{C}$  NMR (101 MHz, DMSO)  $\delta = 166.1$ , 160.1, 158.4, 156.2, 149.0, 147.8, 142.1, 133.9, 129.4, 125.3, 124.5, 124.1, 103.8, 23.5. LC-MS (ESI+):  $R_T = 0.417$  min, 96% at 215 and 254 nm,  $m/z = 287.4$  [M + H] $^+$ . HR-MS (TOF, ESI+): for  $\text{C}_{14}\text{H}_{10}\text{N}_2\text{O}_3\text{S}$  [M], calc'd 287.0485 [M + H] $^+$ , found 287.0485.

**Step 2.** To a solution of carboxylic acid (6.00 mg, 21.0  $\mu\text{mol}$ ) in DMF (0.30 mL) was added *N,N*-diisopropylethylamine (9  $\mu\text{L}$ , 52.4  $\mu\text{mol}$ ), HATU (15.9 mg, 41.8  $\mu\text{mol}$ ), and 5-fluoropyridin-2-ylmethanamine (2.91 mg, 23.1  $\mu\text{mol}$ ), and the reaction was heated at 60 °C. After 3 h, the reaction was removed from the heat, and once it was at room temperature, it was filtered and directly purified by reverse phase HPLC (10–40% over 4 min, Method 1) to afford the title compound as an off-white residue (6.20 mg, 15.4  $\mu\text{mol}$ , 74% yield).  $^1\text{H}$  NMR (400 MHz,  $\text{CDCl}_3$ )  $\delta = 8.86$  (t,  $J = 6.1$  Hz, 1H), 8.46–8.42 (m, 2H), 7.84 (d,  $J = 5.5$  Hz, 1H), 7.58 (d,  $J = 5.5$  Hz, 1H), 7.47 (s, 1H), 7.44 (dd,  $J = 8.5$ , 2.9 Hz, 1H), 7.39–7.34 (m, 2H), 7.26 (d,  $J = 8.4$  Hz, 1H), 4.75 (d,  $J = 6.0$  Hz, 2H), 2.63 (s, 3H).  $^{13}\text{C}$  NMR (101 MHz,  $\text{CDCl}_3$ )  $\delta = 164.6$ , 161.0, 158.9 (d,  $J = 255.2$  Hz), 157.9, 156.4, 153.3 (d,  $J = 3.9$  Hz), 150.5, 148.3, 142.2, 137.6 (d,  $J = 23.9$  Hz), 132.3, 129.3, 125.3, 125.1, 124.5, 123.7 (d,  $J = 18.5$  Hz), 123.1 (d,  $J = 4.3$  Hz), 102.2, 44.5 (d,  $J = 1.6$  Hz), 23.9. LC-MS (ESI+):  $R_T = 0.752$  min,  $>98\%$  at 215 and 254 nm,  $m/z = 395.3$  [M + H] $^+$ . HR-MS (TOF, ESI+): for  $\text{C}_{20}\text{H}_{15}\text{FN}_4\text{O}_2\text{S}$  [M], calc'd 395.0973 [M + H] $^+$ , found 395.0976.

#### 7-Chloro-*N*-(5-fluoropyridin-2-yl)methylthieno[3,2-*b*]pyridine-5-carboxamide (25)

**Step 1.** A mixture of compound 15 (100 mg, 0.514 mmol) and concentrated HCl (37% aqueous, 0.850 mL, 10.2 mmol) was heated to 100 °C. After 1 h, the reaction was removed from the heat and concentrated under reduced pressure to provide the carboxylic acid intermediate, which was used in the following step assuming quantitative yield and without further purification.

**Step 2.** To a solution of carboxylic acid (0.514 mmol) in DMF (2.0 mL) were added *N,N*-diisopropylethylamine (0.224 mL), HATU (391



mg, 1.03 mmol), and (5-fluoropyridin-2-yl)methanamine (71.2 mg, 0.565 mL), and the reaction was heated to 60 °C. After 3 h, the reaction was removed from the heat, diluted with water and dichloromethane once it was at room temperature, and passed through a phase separator with washing with dichloromethane (3X), and the combined organic phases were concentrated by drying. The crude product was purified by silica-gel column chromatography (0–50% EtOAc/hexanes) to afford the title compound as a white solid (99.2 mg, 0.277 mmol, 55% yield). <sup>1</sup>H NMR (400 MHz, CDCl<sub>3</sub>) δ = 8.87 (t, J = 5.8 Hz, 1H), 8.46 (t, J = 1.8 Hz, 1H), 8.23 (s, 1H), 7.88 (d, J = 5.5 Hz, 1H), 7.60 (d, J = 5.5 Hz, 1H), 7.40 (d, J = 2.3 Hz, 1H), 7.39 (d, J = 1.8 Hz, 1H), 4.81 (dd, J = 5.9, 1.0 Hz, 2H). <sup>13</sup>C NMR (101 MHz, CDCl<sub>3</sub>) δ = 164.1, 158.9 (d, J = 255.2 Hz), 156.0, 153.1 (d, J = 3.9 Hz), 149.1, 139.6, 137.6 (d, J = 24.0 Hz), 135.5, 132.9, 125.7, 123.9 (d, J = 18.5 Hz), 123.2 (d, J = 4.3 Hz), 117.4, 44.4 (d, J = 1.6 Hz). LC-MS (ESI+): R<sub>T</sub> = 0.844 min, 90% at 215 nm and 92% at 254 nm, m/z = 322.2 [M + H]<sup>+</sup>. HR-MS (TOF, ESI+): for C<sub>14</sub>H<sub>9</sub>ClFN<sub>3</sub>OS [M], calc'd 322.0212 [M + H]<sup>+</sup>, found 322.0212.

#### N-((5-fluoropyridin-2-yl)methyl)-7-(pyridin-3-yloxy)thieno[3,2-b]pyridine-5-carboxamide (28d, VU6044766)

To a reaction vial under an atmosphere of nitrogen were added 3-pyridinol (8.7 mg, 91.4 μmol) and DMSO (0.300 mL), followed by potassium tert-butoxide (10.2 mg, 91.4 μmol). After 15 min at room temperature, 25 (15.0 mg, 45.7 μmol) in DMSO (0.100 mL) was added, and the reaction was heated to 70 °C. After 16 h, the reaction was removed from the heat, filtered, and directly purified by reverse-phase HPLC (25–55%, Method 2) to provide the title compound as a white residue (8.2 mg, 21.1 μmol, 46% yield). <sup>1</sup>H NMR (400 MHz, CDCl<sub>3</sub>) δ = 8.88 (t, J = 5.4 Hz, 1H), 8.62–8.55 (m, 2H), 8.48–8.42 (m, 1H), 7.86 (d, J = 5.5 Hz, 1H), 7.60 (d, J = 5.5 Hz, 1H), 7.56 (ddd, J = 8.3, 2.8, 1.4 Hz, 1H), 7.52 (s, 1H), 7.44 (ddd, J = 8.4, 4.7, 0.7 Hz, 1H), 7.41–7.34 (m, 2H), 4.77 (d, J = 6.0 Hz, 2H). <sup>13</sup>C NMR (101 MHz, CDCl<sub>3</sub>) δ = 164.5, 160.5, 158.9 (d, J = 255.2 Hz), 158.0, 153.2 (d, J = 3.8 Hz), 150.6, 150.6, 146.9, 142.9, 137.5 (d, J = 24.1 Hz), 132.5, 128.8, 125.4, 125.3, 124.9, 123.9 (d, J = 18.4 Hz), 123.2 (d, J = 4.3 Hz), 102.6, 44.4. LC-MS (ESI+): R<sub>T</sub> = 0.750 min, > 98% at 215 and 254 nm, m/z = 381.0 [M + H]<sup>+</sup>. HR-MS (TOF, ESI+): for C<sub>19</sub>H<sub>13</sub>FN<sub>4</sub>O<sub>2</sub>S [M], calc'd 381.0816 [M + H]<sup>+</sup>, found 381.0819.

#### ■ ASSOCIATED CONTENT

##### SI Supporting Information

The Supporting Information is available free of charge at <https://pubs.acs.org/doi/10.1021/acsbimedchemau.1c00024>.

Experimental procedures and spectroscopic data for selected compounds, detailed pharmacology and DMPK methods (PDF)

#### ■ AUTHOR INFORMATION

##### Corresponding Author

**Craig W. Lindsley** – Warren Center for Neuroscience Drug Discovery, Department of Pharmacology, and Vanderbilt Institute of Chemical Biology, Vanderbilt University, Nashville, Tennessee 37232, United States; [orcid.org/0000-0003-0168-1445](https://orcid.org/0000-0003-0168-1445); Phone: 615-322-8700; Email: [craig.lindsley@vanderbilt.edu](mailto:craig.lindsley@vanderbilt.edu); Fax: 615-343-3088

##### Authors

**Lisa Barbaro** – Warren Center for Neuroscience Drug Discovery and Department of Pharmacology, Vanderbilt University, Nashville, Tennessee 37232, United States

**Alice L. Rodriguez** – Warren Center for Neuroscience Drug Discovery and Department of Pharmacology, Vanderbilt University, Nashville, Tennessee 37232, United States

**Ashlyn N. Blevins** – Warren Center for Neuroscience Drug Discovery and Department of Pharmacology, Vanderbilt

University, Nashville, Tennessee 37232, United States;

[orcid.org/0000-0002-9857-2474](https://orcid.org/0000-0002-9857-2474)

**Jonathan W. Dickerson** – Warren Center for Neuroscience Drug Discovery and Department of Pharmacology, Vanderbilt University, Nashville, Tennessee 37232, United States

**Natasha Billard** – Warren Center for Neuroscience Drug Discovery and Department of Pharmacology, Vanderbilt University, Nashville, Tennessee 37232, United States

**Olivier Boutaud** – Warren Center for Neuroscience Drug Discovery and Department of Pharmacology, Vanderbilt University, Nashville, Tennessee 37232, United States

**Jerri L. Rook** – Warren Center for Neuroscience Drug Discovery and Department of Pharmacology, Vanderbilt University, Nashville, Tennessee 37232, United States

**Colleen M. Niswender** – Warren Center for Neuroscience Drug Discovery, Department of Pharmacology, Department of Chemistry, and Vanderbilt Brain Institute, Vanderbilt University, Nashville, Tennessee 37232, United States; Vanderbilt Kennedy Center, Vanderbilt University Medical Center, Nashville, Tennessee 37232, United States

**P. Jeffrey Conn** – Warren Center for Neuroscience Drug Discovery, Department of Pharmacology, and Vanderbilt Institute of Chemical Biology, Vanderbilt University, Nashville, Tennessee 37232, United States; Vanderbilt Kennedy Center, Vanderbilt University Medical Center, Nashville, Tennessee 37232, United States

**Darren W. Engers** – Warren Center for Neuroscience Drug Discovery and Department of Pharmacology, Vanderbilt University, Nashville, Tennessee 37232, United States

Complete contact information is available at:

<https://pubs.acs.org/10.1021/acsbimedchemau.1c00024>

#### Funding

This work was generously supported by the Warren Family and Foundation for establishing the William K. Warren, Jr. Chair in Medicine (C.W.L.) and for endowing the Warren Center for Neuroscience Drug Discovery.

#### Notes

The authors declare no competing financial interest.

#### ■ ABBREVIATIONS

mGlu<sub>5</sub>, metabotropic glutamate receptor subtype 5; CRC, concentration–response-curve; NAM, negative allosteric modulator; PAM, positive allosteric modulator; PBL, plasma:brain level; SAR, structure–activity-relationships

#### ■ REFERENCES

- Wotten, D.; Christopoulos, C.; Marti-Solano, M.; Babu, M. M.; Sexton, P. M. Mechanisms of signalling and biased agonism in G protein-coupled receptors. *Nat. Rev. Mol. Cell Biol.* **2018**, *19*, 638–653.
- Hilger, D.; Masureel, M.; Kobilka, B. K. Structure and dynamics of GPCR signaling complexes. *Nat. Struct. Mol. Biol.* **2018**, *25*, 1–34.
- Hauser, A. S.; Attwood, M. M.; Rask-Andersen, M.; Schioth, H. B.; Gloriam, D. E. Trends in GPCR drug discovery: new agents, targets and indications. *Nat. Rev. Drug Discovery* **2017**, *16*, 829–842.
- Niswender, C. M.; Conn, P. J. Metabotropic glutamate receptors: physiology, pharmacology, and disease. *Annu. Rev. Pharmacol. Toxicol.* **2010**, *50*, 295–322.
- Conn, P. J.; Christopoulos, A.; Lindsley, C. W. Allosteric Modulators of GPCRs as a Novel Approach to Treatment of CNS Disorders. *Nat. Rev. Drug Discovery* **2009**, *8*, 41–54.
- Melancon, B. J.; Hopkins, C. R.; Wood, M. R.; Emmitte, K. A.; Niswender, C. M.; Christopoulos, A.; Conn, P. J.; Lindsley, C. W.

Allosteric Modulation of 7 Transmembrane Spanning Receptors: Theory, Practice and Opportunities for CNS Drug Discovery. *J. Med. Chem.* **2012**, *55*, 1445–1464.

(7) Wenthur, C. J.; Gentry, P. R.; Mathews, T. P.; Lindsley, C. W. Drugs for allosteric sites on receptors. *Annu. Rev. Pharmacol. Toxicol.* **2014**, *54*, 165–184.

(8) Conn, P. J.; Lindsley, C. W.; Meiler, J.; Niswender, C. M. Opportunities and challenges in the discovery of allosteric modulators of GPCRs for the treatment of CNS disorders. *Nat. Rev. Drug Discovery* **2014**, *13*, 692–708.

(9) Lindsley, C. W.; Emmitte, K. A.; Hopkins, C. R.; Bridges, T. M.; Gregory, K. A.; Niswender, C. M.; Conn, P. J. Practical strategies and concepts in GPCR allosteric modulator discovery: Recent advances with metabotropic glutamate receptors. *Chem. Rev.* **2016**, *116*, 6707–6741.

(10) Sharma, S.; Kedrowski, J.; Rook, J. M.; Smith, J. M.; Jones, C. K.; Rodriguez, A. L.; Conn, P. J.; Lindsley, C. W. Discovery of Molecular Switches that Modulate Modes of mGluR5 Pharmacology *In Vitro* and *In Vivo* Within a Series of Functionalized 5-(phenylethynyl)-pyrimidines. *J. Med. Chem.* **2009**, *52*, 4103–4106.

(11) Lindsley, C. W.; Philip, S. Portuguese Medicinal Chemistry Lectureship: Drug Discovery Targeting Allosteric Sites. *J. Med. Chem.* **2014**, *57*, 7485–7498 2013.

(12) Wood, M. R.; Hopkins, C. R.; Brogan, J. T.; Conn, P. J.; Lindsley, C. W. 'Molecular switches' on allosteric ligands that modulate modes of pharmacology. *Biochemistry* **2011**, *50*, 2403–2410.

(13) Wenthur, C. J.; Niswender, C. M.; Morrison, R.; Daniels, J. S.; Conn, P. J.; Lindsley, C. W. Discovery of (R)-(2-fluoro-4-((4-methoxyphenyl)ethynyl)phenyl)(3-hydroxypiperidin-1-yl)methanone (ML337), an mGlu<sub>3</sub> selective and CNS penetrant negative allosteric modulator (NAM). *J. Med. Chem.* **2013**, *56*, 3713–3718.

(14) Engers, J. L.; Rodriguez, A. L.; Konkol, L. C.; Morrison, R. D.; Thompson, A. D.; Byers, F. W.; Blobaum, A. L.; Chang, S.; Loch, M. T.; Niswender, C. M.; Daniels, J. S.; Jones, C. K.; Conn, P. J.; Lindsley, C. W.; Emmitte, K. A. Discovery of VU0650786: A selective and CNS penetrant negative allosteric modulator of metabotropic glutamate receptor subtype 3 with antidepressant and anxiolytic activity in rodents. *J. Med. Chem.* **2015**, *58*, 7485–7500.

(15) Evans, B. E.; Rittle, K. E.; Bock, M. G.; DiPardo, R. M.; Freidinger, R. M.; Whitter, W. L.; Lundell, G. F.; Veber, D. F.; Anderson, P. S.; Chang, R. S. L.; Lotti, V. J.; Cerino, D. J.; Chen, T. B.; Kling, P. J.; Kunkel, K. A.; Springer, J. P.; Hirshfield, J. Methods for drug discovery: development of potent, selective, orally effective cholecystokinin antagonists. *J. Med. Chem.* **1988**, *31*, 2235–2246.

(16) Davis, D. C.; Bungard, J. D.; Chang, S.; Rodriguez, A. L.; Blobaum, A. L.; Boutaud, O.; Melancin, B. J.; Niswender, C. M.; Conn, P. J.; Lindsley, C. W. Lead optimization of the VU0486321 series of mGlu<sub>1</sub> PAMs. Part 4: SAR reveals positive cooperativity across multiple mGlu receptor subtypes leading to subtype unselective PAMs. *Bioorg. Med. Chem. Lett.* **2021**, *37*, 127724.

(17) Berizzi, A. E.; Bender, A. M.; Conn, P. J.; Lindsley, C. W.; Sexton, P. M.; Langmead, C. J.; Christopoulos, A. Structure-activity relationships of pan-G<sub>q/11</sub> coupled muscarinic acetylcholine receptor positive allosteric modulators. *ACS Chem. Neurosci.* **2018**, *9*, 1818–1828.

(18) Bennett, K. A.; Christopher, J. A.; Tehan, B. G. Structure-based discovery and development of metabotropic glutamate receptor 5 negative allosteric modulators. *Adv. Pharmacol.* **2020**, *88*, 35–58.

(19) Arsova, A.; Mollr, T. C.; Hellyer, S. D.; Vedel, L.; Foster, S. R.; Hansen, J. L.; Brauner-Osborn, H.; Gregory, K. J. Positive Allosteric Modulators of Metabotropic Glutamate Receptor 5 as Tool Compounds to Study Signaling Bias. *Mol. Pharmacol.* **2021**, *99*, 328–341.

(20) Emmitte, K. A. mGlu<sub>5</sub> negative allosteric modulators: a patent review (2013–2016). *Expert Opin. Ther. Pat.* **2017**, *27*, 691–706.

(21) Felts, A. S.; Rodriguez, A. L.; Blobaum, A. L.; Morrison, R. D.; Bates, B. S.; Thompson, A. D.; Rook, J. M.; Byers, F. W.; Chang, S.; Venable, D. F.; Luscombe, V. B.; Tamagnan, G. D.; Bridges, T. M.; Niswender, C. M.; Daniels, J. S.; Jones, C. K.; Conn, P. J.; Lindsley, C. W.; Emmitte, K. A. Discovery of N-(5-fluoropyridin-2-yl)-6-methyl-4-

(pyrimidin-5-yloxy)picolinamide (VU0424238): A novel negative allosteric modulator of metabotropic glutamate receptor subtype 5 selected for clinical development. *J. Med. Chem.* **2017**, *60*, 5072–5085.

(22) Rook, J. M.; Xiang, Z.; Lv, X.; Ghosal, A.; Dickerson, J.; Bridges, T. M.; Johnson, K. A.; Bubser, M.; Gregory, K. J.; Vinson, P. N.; Byun, N.; Stauffer, S. R.; Daniels, J. S.; Niswender, C. M.; Lavreysen, H.; Mackie, C.; Conde; Ceide, S.; Alcazar, J.; Bartolome, J. M.; Macdonald, G. J.; Steckler, T.; Jones, C. K.; Lindsley, C. W.; Conn, P. J. Biased mGlu<sub>5</sub> positive allosteric modulators provide *in vivo* efficacy without potentiating mGlu<sub>5</sub> modulation of NMDAR currents. *Neuron* **2015**, *86*, 1029–1040.

(23) Conde-Ceide, S.; Martin-Martin, M. L.; Alcazar, J.; Manka, T.; Tong, H. M.; Garcia-Barrantes, P. M.; Lavreysen, H.; Mackie, C.; Vinson, P. N.; Daniels, S. J.; Menges, A.; Niswender, C. M.; Jones, C. K.; Macdonald, G. J.; Steckler, T.; Conn, P. J.; Stauffer, S. R.; Bartolome-Nebreda, J. M.; Lindsley, C. W. Discovery of VU0409551/JNJ-46778212: An mGlu<sub>5</sub> Positive Allosteric Modulator Clinical Candidate Targeting Schizophrenia. *ACS Med. Chem. Lett.* **2015**, *6*, 716–720.

(24) Engers, J. L.; Childress, E. S.; Long, M. F.; Capstick, R. A.; Luscombe, V. B.; Cho, H. P.; Dickerson, J. W.; Rook, J. M.; Blobaum, A. L.; Niswender, C. M.; Conn, P. J.; Lindsley, C. W. VU6007477, a novel M<sub>1</sub> PAM based on a pyrrolo[2,3-*b*]pyridine carboxamide core devoid of cholinergic side effects. *ACS Med. Chem. Lett.* **2018**, *9*, 917–922.

(25) Zhao, J.; Zhang, D.; Stashko, M. A.; DeRyckere, D.; Vasileiadi, E.; Parker, R. E.; Hunter, D.; Lu, Q.; Zhang, Y.; Norris-Drouin, J.; Li, B.; Drewry, D. H.; Kireev, D.; Graham, D. K.; Earp, H. S.; Frye, S. V.; Wang, X. Highly selective MERTK inhibitors achieved by a single methyl group. *J. Med. Chem.* **2018**, *61*, 10242–10254.

(26) Leung, C. S.; Leung, S. S.; Tirado-Rives, J.; Jorgensen, W. Methyl Effects on Protein–Ligand Binding. *J. Med. Chem.* **2012**, *55*, 4489–4500.

(27) Schonherr, H.; Cernak, T. Profound Methyl Effects in Drug Discovery and a Call for New C–H Methylation Reactions. *Angew. Chem., Int. Ed.* **2013**, *52*, 12256–12267.

(28) For information see: <https://clinicaltrials.gov/ct2/show/NCT03220295>, accessed 07/09/2021.

(29) See [Supporting Information](#) for full details.

#### ■ NOTE ADDED AFTER ASAP PUBLICATION

The uncorrected version posted ASAP on August 20, 2021; the correct version reposted on August 24, 2021.